ORNL/TM-13759
SNS/TSR-0097

OAK RIDGE NATIONAL LABORATORY

LOCKHEED MARTIN

Screening Test Results of Fatigue Properties of Type 316LN Stainless Steel in Mercury

S. J. Pawel
J. R. DiStefano
J. P. Strizak
C. O. Stevens
E. T. Manneschmidt

MANAGED AND OPERATED BY
LOCKHEED MARTIN ENERGY RESEARCH CORPORATION
FOR THE UNITED STATES
DEPARTMENT OF ENERGY

ORNL-27 (3-96)

ORNL/TM-13759
SNS/TSR-0097

SCREENING TEST RESULTS OF FATIGUE PROPERTIES OF TYPE 316LN STAINLESS STEEL IN MERCURY

S. J. Pawel, J. R. DiStefano, J. P. Strizak, C. O. Stevens, and E. T. Manneschmidt

Date Published: March 1999

Prepared for the
U.S. Department of Energy
Spallation Neutron Source
SNS/TSR-0097

Prepared by the
OAK RIDGE NATIONAL LABORATORY
Oak Ridge, Tennessee 37831-6285
managed by
Lockheed Martin Energy Research Corporation
for the
U.S. DEPARTMENT OF ENERGY
Under contract DE-AC05-96OR22464

CONTENTS

LIST OF FIGURES

PAGE

LIST OF TABLES

PAGE

SCREENING TEST RESULTS OF FATIGUE PROPERTIES OF TYPE 316LN STAINLESS STEEL IN MERCURY*

S. J. Pawel, J. R. DiStefano, J. P. Strizak, C. O. Stevens, and E. T. Manneschmidt

ABSTRACT

Fully reversed, load-controlled uniaxial push-pull fatigue tests at room temperature have been performed in air and in mercury on specimens of type 316LN stainless steel. The results indicate a significant influence of mercury on fatigue properties. Compared to specimens tested in air, specimens tested in mercury had reproducibly shorter fatigue lives (by a factor of 2-3), and fracture faces exhibiting intergranular cracking. Preliminary indications are that crack initiation in each environment is similar, but mercury significantly accelerates crack propagation.

1. INTRODUCTION

The target material for the Spallation Neutron Source (SNS) will be liquid mercury contained in a 316LN austenitic stainless steel vessel. Experiments are underway to determine whether the container material is susceptible to liquid metal embrittlement (LME). LME occurs when the ductility of a stressed solid is decreased by the growth of cracks that form at or near the surface wetted by the liquid metal. Experimental observations have indicated this can occur by several processes: grain boundary decohesion, selective corrosive attack, and, more classically, no chemical or structural modification before formation and growth of a crack. Most studies emphasize the requirement of a tensile stress and some degree of chemical wetting for LME to occur.

Mercury is known to embrittle certain materials; for example, aluminum, brass, and some nickel-base alloys [1] are embrittled as noted in Table 1. In addition, at least one study has shown evidence of LME of type 304L SS in mercury [2] as indicated in Table 2. (Note, however, that type 316L SS was apparently not susceptible to LME in this latter study.)

*Research sponsored by the U.S. Department of Energy, Spallation Neutron Source

SNS/TSR-0097

Table 1. Tensile fracture characteristics of Ni and Ni-Alloys in mercury at room temperature [1].

Material	Air	Mercury
Ni-200 (commercially pure Ni)	All alloys had ductile cup & cone fractures subsequent to necking. Fracture from microvoid coalescence	Brittle fracture
Monel 400		Complete intergranular embrittlement at low strain rates
Inconel 600		Similar to Ni-200
Inconel 625		Similar to Monel 400
Inconel 718		Intermediate between Ni-200 and Monel 400. Noticeable embrittlement with intergranular failure
Alloy 800/825		Not embrittled; cup & cone failure after necking. (Later fatigue tests showed intergranular cracking)

C9900254-20

Table 2. Effect of mercury environment on slow strain rate tests (5×10^{-6}/sec) at room temperature [2].

Material	Environment	Time to Failure (h)	Reduction in Area (%)	Comments
304L SS	Air	33	83	No cracking
	Mercury	28	49	Linear cracking
316L SS	Air	37	80	No cracking
	Mercury	38	79	No cracking
Alloy 600	Air	29	72	Linear/Random cracking
	Mercury	24	58	Linear/Random cracking
Alloy 800	Air	24	77	No cracking
	Mercury	26	71	No cracking

C9900254-21

At the beginning of the SNS Research and Development program for target materials, constant extension rate tests of type 316 SS were conducted in air and mercury [3]. As indicated in Fig. 1, these tests did not reveal any effect of the mercury environment (compared to air) on the room temperature tensile properties of 316 SS in any of several heat treatment conditions. It was noted, however, that the fresh fracture surface of specimens tested in Hg was invariably wetted by the Hg while the rest of the specimen was not wetted.

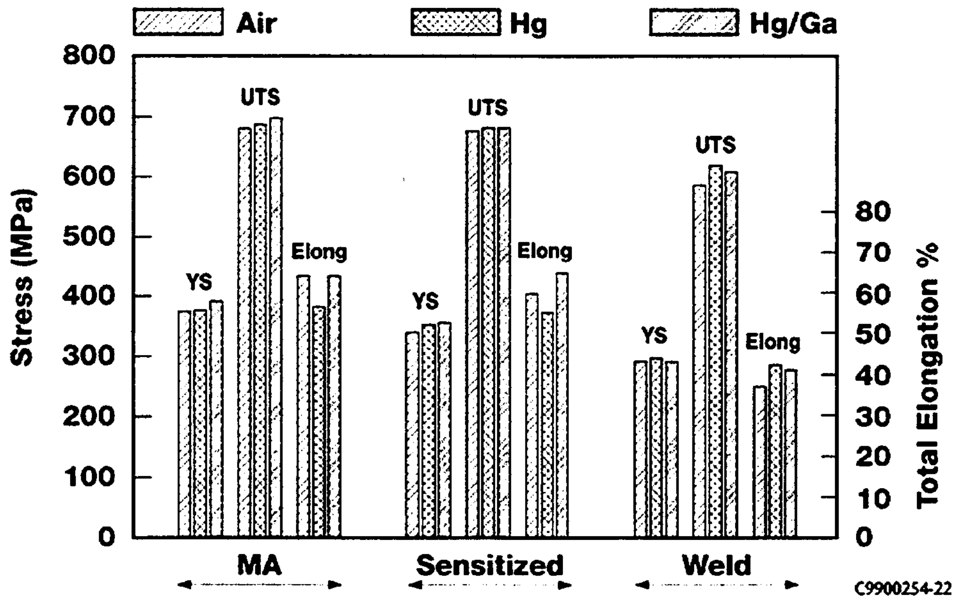

Fig. 1. Room temperature tensile properties of type 316 SS as a function of heat treatment and test environment. The Hg/Ga environment was pure Hg with 0.5% Ga added.

In contrast with standard uniaxial tensile tests in which the specimens typically fail in a single fast fracture after plastic deformation (necking) has accommodated the maximum load, fatigue failure often generates one or more cracks open to the specimen surface that propagate as the cyclic loading continues. If such a crack is wet by liquid mercury, the potential for LME is enhanced.

The SNS target vessel will be subjected to an extremely high number of thermal transients and dynamic pressure loads while it is in contact with mercury. As a result, studies to examine potential LME effects for type 316LN SS in mercury under cyclic loading conditions have been initiated. The purpose of this report is to document the results of some initial screening tests of 316LN fatigue properties in mercury.

2. EXPERIMENTAL

A single heat of mill-annealed type 316LN SS material was used for all of the screening tests. The 25-mm thick plate from which the specimens were machined met the American Society for Testing and Materials (ASTM) specification A240-88C. The composition and relevant physical and mechanical properties of this material appear in Table 3. Additional information regarding the general microstructure, tensile properties, and strain-controlled low-cycle fatigue properties is recorded elsewhere [4].

Fatigue test specimens (see Fig. 2) were machined parallel to the primary rolling direction of the 25-mm plate. Since the gage diameter of the specimen size selected for these screening tests was somewhat smaller than that employed for the data developed by Swindeman[4], i.e., 5.1 mm compared to 6.3 mm, a limited number of fully reversed, strain controlled fatigue tests were conducted in air to assure no specimen size effect would be encountered. Results of these tests are plotted in Fig. 3 and show no effect of specimen diameter. Figure 3 also shows the fatigue design curve from Section III of the American Society of Mechanical Engineers (ASME) Boiler and Pressure Vessel Code for type 316L. These strain-controlled tests provided guidance in selecting test parameters for the room temperature fully reversed load-controlled tests conducted to investigate LME effects of mercury on the SNS target material.

Table 3. Vendor ladle analysis for Jessop Steel Company heat 18474 type 316LN stainless steel. Selected physical and mechanical properties for the mill annealed material also included.

Element	Weight Percent
C	0.009
Mn	1.75
P	0.029
S	0.002
Si	0.39
Ni	10.2
Cr	16.31
Mo	2.07
Co	0.16
Cu	0.23
N	0.11
Fe	balance

Room temperature properties (test at strain rate 8×10^{-5}/s)	
0.2% offset yield strength	259.1 MPa
ultimate tensile strength	587.5 MPa
elongation	86.2%
reduction in area	88.1%
grain size	ASTM 3.7

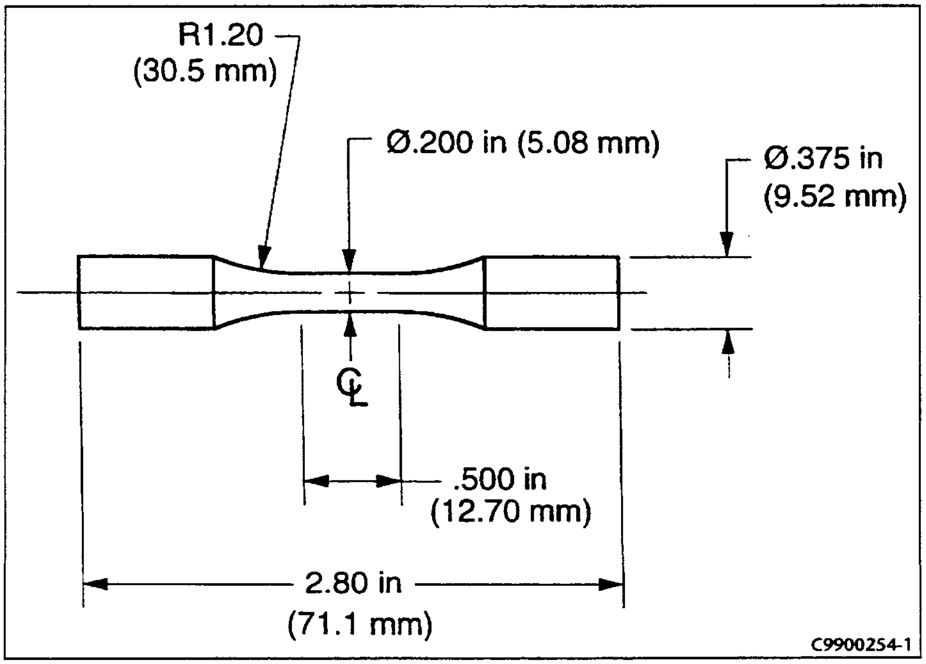

Fig. 2. Fatigue specimen dimensions. Specimens fabricated utilizing low stress grinding, blended radii, and polished gage section.

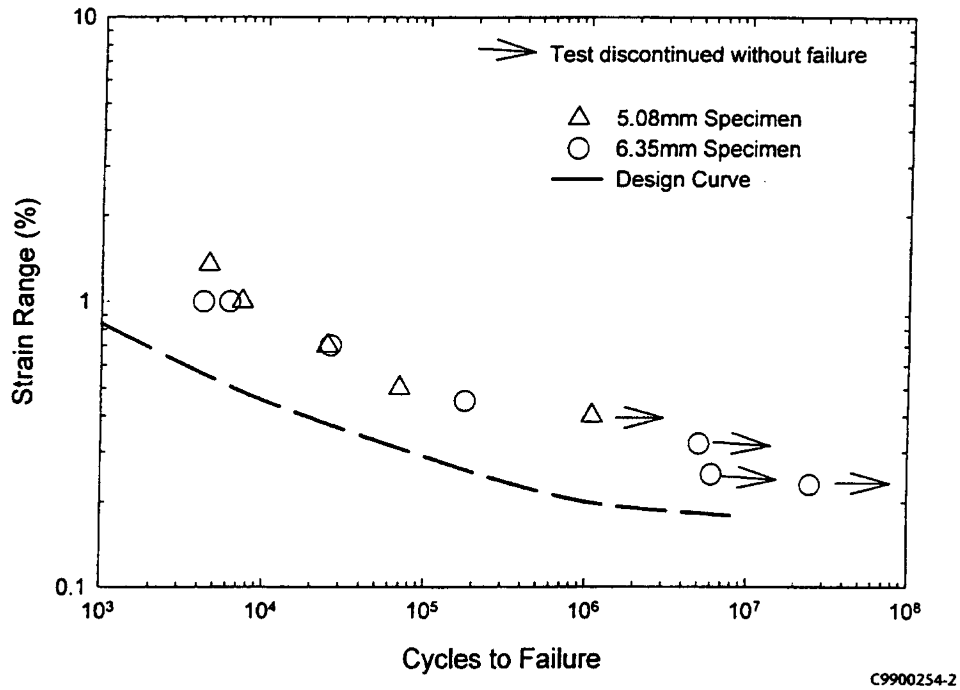

Fig. 3. Room temperature fatigue data for tests in air on mill annealed 316LN used in this study.

To hold Hg around the gage section of the specimen during testing, press-fit bushings fabricated from commercially pure nickel were designed to fit the ends of the fatigue specimens. Figure 4 includes a cut-away of the bushing design that comprises the primary "mercury containment system." The bushing on the lower half of the specimen extends from the extreme bottom to just above the top end of the gage section, forming a cup around the gage section. The wall thickness of the cup was thinned somewhat to increase the volume of mercury that could be contained in the annular region between bushing and specimen. The top end of the specimen was fitted with a bushing with the same outside diameter as the lower half to facilitate gripping in the fatigue machine. The entire assembly was loaded into the fatigue machine surrounded by a large plastic bag to contain any mercury that might tend to be dislodged from the cup as the specimen fractured.

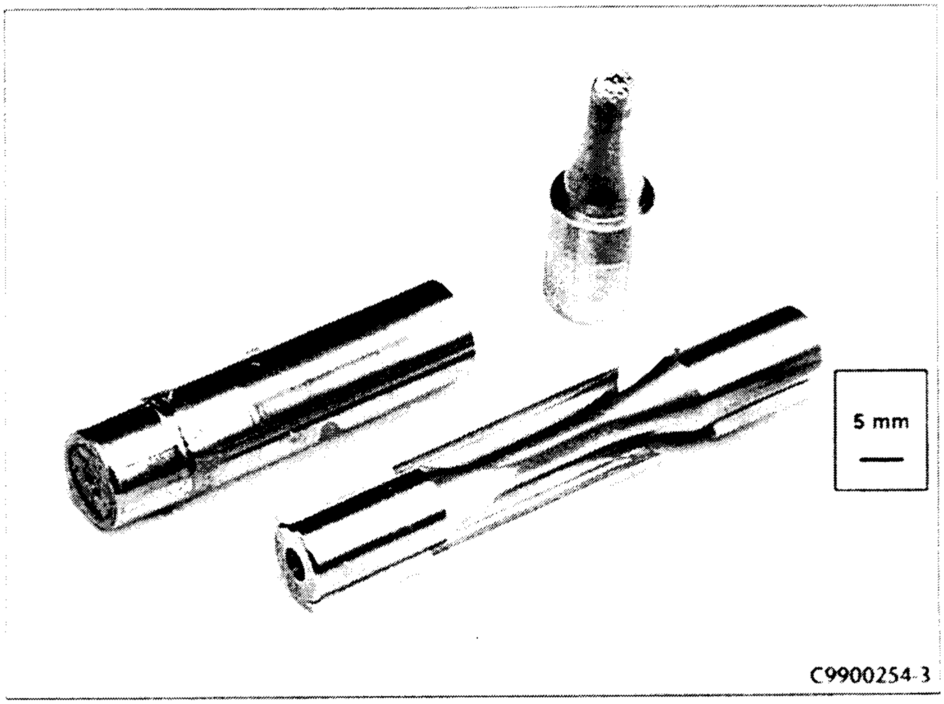

Fig. 4. Fatigue specimen with press-fit bushings to facilitate gripping and mercury containment

Specimens of "bare" 316LN SS were tested at room temperature with the mercury container empty as well as with the gage section immersed in mercury. In addition, a limited number of fatigue specimens on which a thin layer of silver solder had been deposited on the gage section were also tested with the gage section immersed in mercury. The solder was applied by fixing the specimens in a vice and swabbing a liquid fluxing agent (known industrially as Ruby Flux; a mixture of hydrochloric acid and zinc chloride) while preheating the gage length with a hot air gun. Subsequently, a standard soldering iron was used to apply the silver solder (composition approximately 97% Pb, 2% Ag, 1% Sn) to the gage section (see Fig. 5). The purpose of the silver solder was to facilitate wetting of the gage section from the very onset of the test. It was found that mercury readily wets this solder at room temperature and quickly (minutes) amalgamates the entire deposit. In principle, this action leaves the mercury in intimate contact with the substrate stainless steel, which is relatively free of surface oxide due to the successful fluxing and application of solder.

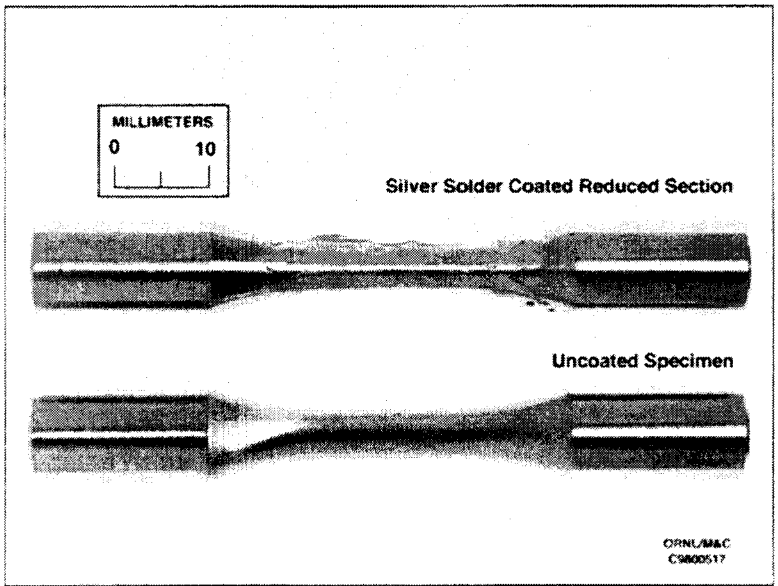

Fig. 5. SNS fatigue specimens with and without solder coating.

The uniaxial fatigue tests were performed with fully reversed loading (tension and compression to the maximum stress). The loading frequency varied slightly for different loads but was in the range of 0.2 to 0.5 Hz for all tests except that at the lowest stress (2.0 Hz to accumulate a large number of cycles in a relatively short time). The test procedure, including due consideration for specimen alignment, followed ASTM E606.

3. RESULTS AND DISCUSSION

Fig. 6 summarizes the preliminary data collected to date. At several stresses above the apparent fatigue limit, the data (which include several duplicate tests) indicate that exposure to mercury (with or without the silver soldered gage section) reproducibly decreases the cycles to failure by a factor of 2-3 compared to the equivalent test in air.

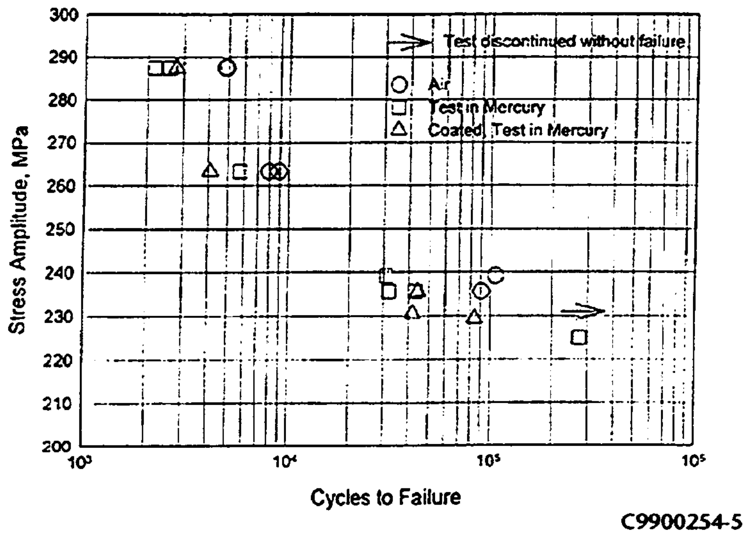

Fig. 6. Room temperature 316LN fatigue data as a function of test environment. Fully reversed stress controlled tests; R=-1.

For each specimen exposed to mercury, the post-test fracture surfaces were essentially wetted completely by the mercury while other surfaces were not wetted (see Fig. 4 for an example). Longitudinal sections cut from the fracture specimens were examined metallographically and found to be mostly smooth and featureless at the outer edges except for the rough edge defining the fracture surface. However, specimens tested at the highest stress (lowest number of cycles to failure) revealed some secondary cracking. Representative of the specimens tested at 287 MPa (41.7 ksi) in air, Fig. 7 shows 4-5 shallow cracks in close proximity to the failure site. Figure 8, representing the specimens tested at the same stress in Hg, shows a similar number of secondary cracks along the gage length – however, these secondary cracks are very long and exhibit some intergranular character. At face value, this comparison suggests that crack initiation phenomena in each environment (air vs. Hg) are similar, but there is far less resistance to crack propagation in the Hg environment.

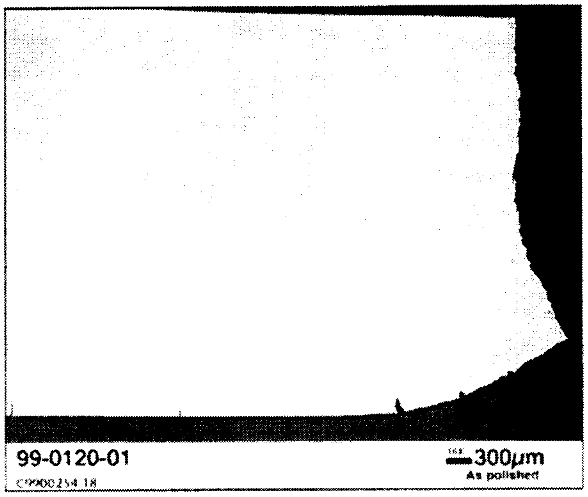

Fig. 7. As-polished longitudinal cross section of 316LN fatigue specimen tested in air at room temperature (287 MPa, 4935 cycles to failure).

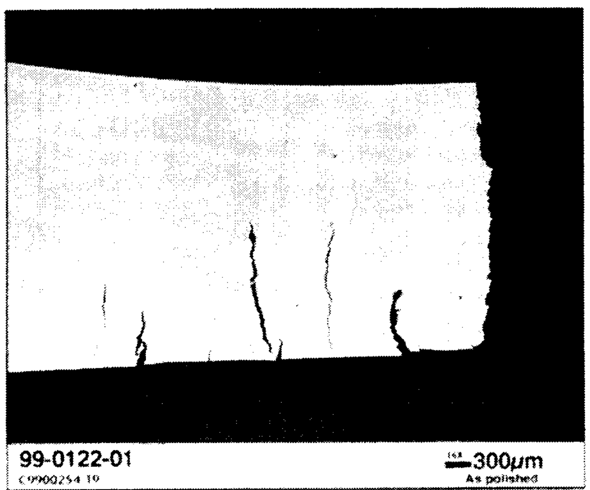

Fig. 8. As-polished longitudinal cross section of 316LN fatigue specimen tested in Hg at room temperature (287 MPa, 2572 cycles to failure).

Fracture faces were also examined in the scanning electron microscope (SEM). Figure 9 shows representative views of the fracture surface of a specimen tested in air at 287 MPa. These photographs reveal typical fatigue striations across the entire surface with short, shallow cracks essentially parallel to the striations in a few locations. Largely, the fracture reveals very little surface relief or typical signs of ductility (such as void coalescence), although the extreme edge of the specimen (Fig. 10) reveals a location of ductile overload (final failure site).

Figure 11 shows the typical fracture surface of the specimens tested in Hg at the highest stress. In contrast with the specimen tested in air, the fracture surface here appears much more brittle with widespread intergranular cracking. In general, fatigue striations are subtle and difficult to resolve, although they are occasionally visible on the grain faces. The brittle appearance and multiple, branching cracks suggest LME is occurring in specimens tested in mercury.

At lower stress, the fracture surfaces of the specimens tested in air and in mercury become more similar in that striations are more obvious on specimens tested in Hg and the amount of cracking (in both environments) generally decreases. However, various degrees of intergranular cracking are consistently observed on the fractures of specimens tested in mercury (see Fig. 12).

At present, it appears that mercury has a significant effect on fatigue properties and relatively little effect on standard tensile properties due to crack propagation and wetting-related phenomena. In fatigue, cracks typically initiate in one or more locations on the surface of the specimen. When these cracks open in air, the crack faces quickly develop a protective oxide and propagation of the crack depends on the state of stress and physical characteristics of the bulk specimen. However, when these cracks open in a mercury environment, the fresh fracture faces are wetted by the mercury. Crack propagation then depends upon the interaction of the mercury with the material (particularly grain boundaries) in addition to the bulk properties of the material. In a standard tensile-type test, however, cracks on the surface do not appear until at/near end-of-test. As a result, there is little opportunity for mercury to influence the result.

These preliminary fatigue test results indicate there is cause to pursue a more complete understanding of the interaction of 316LN and mercury in a fatigue-type environment. The data base should be expanded to include different loading conditions (other than fully reversed loading, which is not prototypic to expected target conditions) and some effort made to define the fatigue limit for 316LN in mercury.

(a)

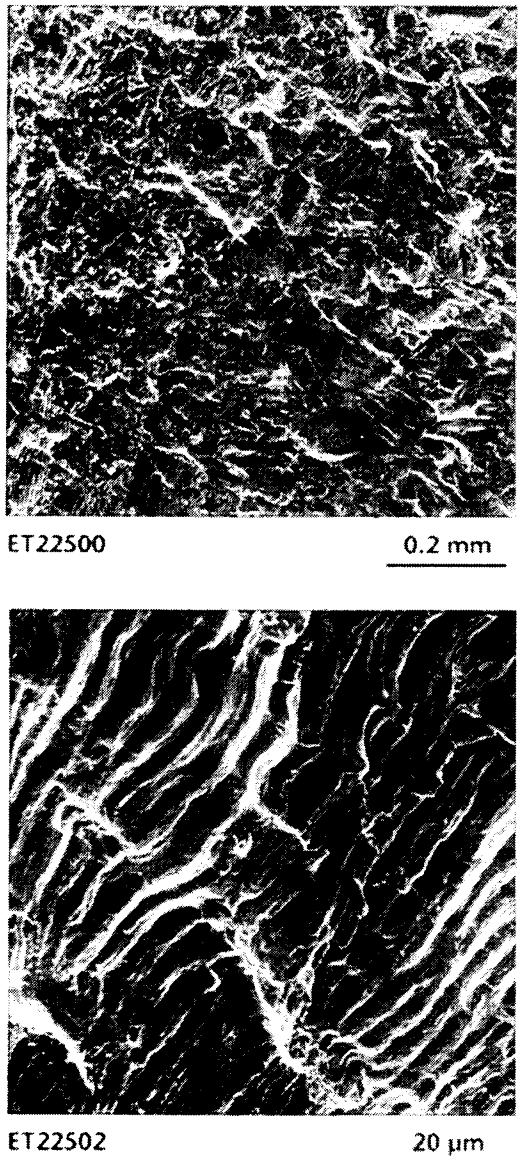

(b)

Fig. 9. Fracture surface of 316LN fatigue specimen tested in air at room temperature (287 MPa, 4935 cycles to failure). Photo (a) is 100X near the specimen center, and (b) is 1000X in the same region.

(a)
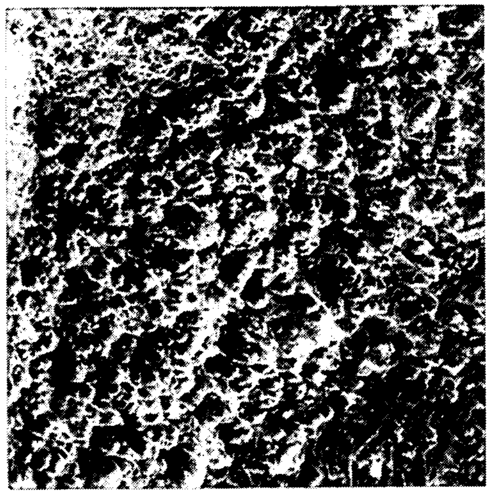

ET22503 0.2 mm

(b)
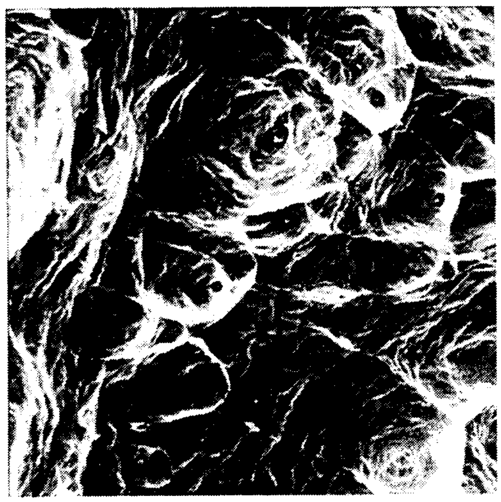

ET22504 20 μm

Fig. 10. Fracture surface of 316LN fatigue specimen tested in air at room temperature (287 MPa, 4935 cycles to failure). Photo (a) is 100X at specimen edge, and (b) is 1000X in the same region.

(a)
(b)

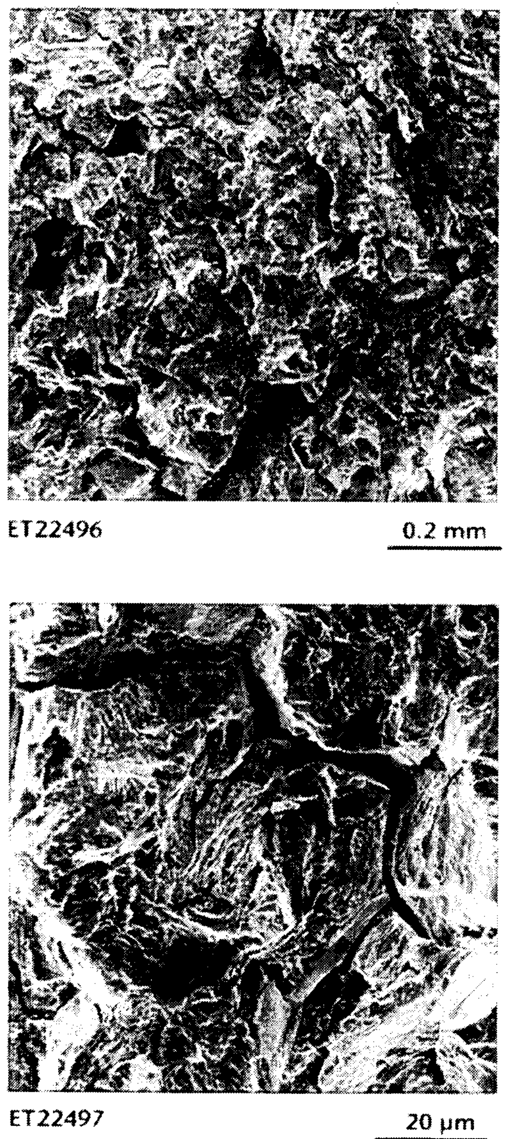

Fig. 11. Fracture surface of 316LN fatigue specimen tested in air at room temperature (287 MPa, 2572 cycles to failure). Photo (a) is 100X near the specimen center, and (b) is 1000X in the same region.

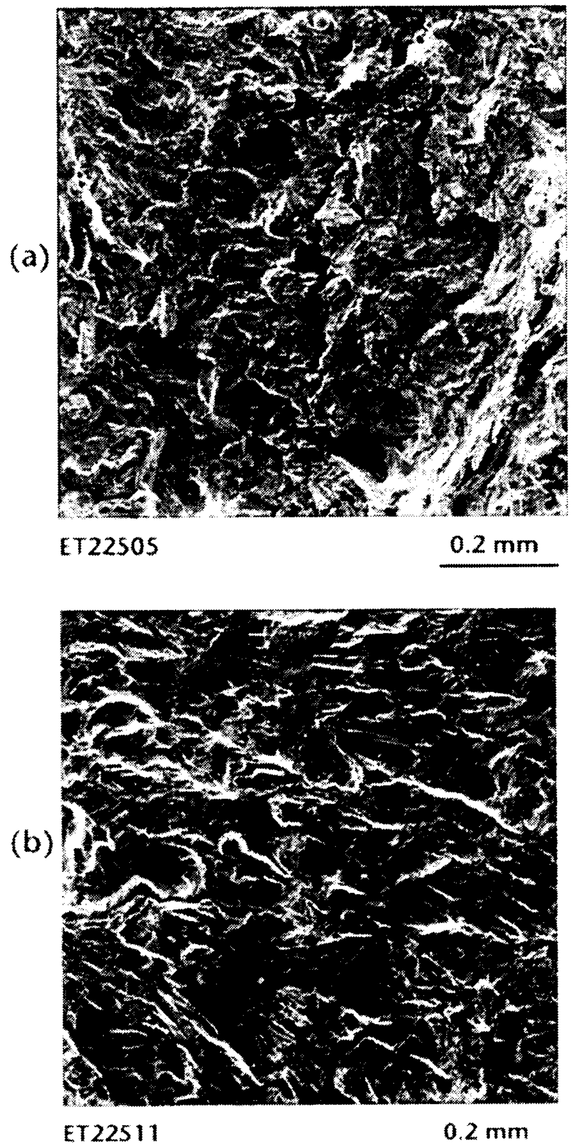

Fig. 12. Fracture surfaces of 316LN fatigue specimens tested in Hg at room temperature. Photo (a) is 100X near the specimen center tested at 239 MPa (30,851 cycles to failure), and (b) is 100X of specimen center tested at 236 MPa (43,136 cycles to failure).

4. REFERENCES

1. **C. E. Price and J. K. Good**, "The Tensile Fracture Characteristics of Nickel, Monel, and Selected Superalloys Broken in Liquid Mercury," ASME Journal of Engineering Materials and Technology, Vol. 106, p.184 (1984).

2. **J. J. Krupowicz**, "Effect of Heat Treatment on Liquid Metal-Induced Cracking of Austenitic Alloys," Slow Strain Rate Testing for the Evaluation of Environmentally Induced Cracking: Research and Engineering Applications, ASTM STP 1210, R. D. Cane, ed., ASTM, Philadelphia pp. 193-201 (1993).

3. **J. R. DiStefano, S. J. Pawel, and E. T. Manneschmidt**, "Materials Compatibility Studies for the Spallation Neutron Source," ORNL/TM-13675, September 1998.

4. **R. W. Swindeman**, "HWR-NPR Materials/Systems Integrity Mechanical Behavior Report," ORNL/NPR-92/94, Martin Marietta Energy Systems, Inc., Oak Ridge National Laboratory, June 1993.

5. ACKNOWLEDGMENTS

The authors would like to thank K. Farrell and R. W. Swindeman for helpful reviews of the manuscript. In addition, thanks are due to J. R. Mayotte for metallography, D. N. Braski for SEM, and S. A. Shugart for preparation of the manuscript.

INTERNAL DISTRIBUTION

1. R. R. Allen
2. J. R. Alonso
3. B. R. Appleton
4. J. B. Ball
5. R. E. Battle
6. L. A. Charlton
7. K. K. Chipley
8. J. E. Cleaves
9. J. W. Cobb
10. D. F. Craig
11. H. H. Cromwell
12. J. H. DeVan
13—17. J. R. DiStefano
18. K. Farrell
19. T. A. Gabriel
20. J. R. Haines
21. H. W. Hayden
22. L. L. Horton
23. J. D. Hunn
24. D. T. Ingersoll
25. L. L. Jacobs
26. D. R. Johnson
27. J. O. Johnson
28. A. G. Jordan
29. E. H. Lee
30. D. C. Lousteau
31. A. T. Lucas
32. E. T. Manneschmidt
33. L. K. Mansur
34. T. E. Mason
35. T. J. McManamy
36. G. E. Michaels
37. D. E. Moncton
38—42. S. J. Pawel
43. M. J. Rennich
44. S. L. Schrock
45. M. Siman-Tov
46. P. T. Spampianto
47. C. O. Stevens
48. C. N. Strawbridge
49—53. J. P. Strizak
54. R. P. Taleyarkhan
55. C. D. West
56. J. H. Whealton
57. D. K. Wilfert
58. D. F. Wilson
59. G. T. Yahr
60. G. L. Yoder
61. ORNL Central Research Library
62. Document Reference Section
63—64. Laboratory Records, ORNL-RC
65—66. Office of Scientific & Technical Information

EXTERNAL DISTRIBUTION

67. ARGONNE NATIONAL LABORATORY, 9700 South Cass Ave., Building 360, IPNS Division, Argonne, IL 60439
    J. M. Carpenter

68. LOS ALAMOS NATIONAL LABORATORY, LER/ADTT, Los Alamos, NM 87545
    A. Jason
    W. Sommer (MS-E546)

69. Monroe Wechsler, 106 Hunter Hill Place, Chapel Hill, NC 27514-9128

70. BROOKHAVEN NATIONAL LAB0RATORY, Upton,, NY 11973
    W. Weng
    M. Todowso

71. PAUL SCHERRER INSTITUTE, CH-5232, Villigen-PSI, Switzerland
    G. Bauer